Catalysis Letters, Vol. 117, Nos. 3–4, September 2007 (© 2007)
DOI: 10.1007/s10562-007-9130-9

CO_2 addition on the non-oxidative dehydro-aromatization of methane over MoMCM-22

Alexandre Carlos Camacho Rodrigues[a,b,*] and José Luiz Fontes Monteiro[a]

[a]*NUCAT/PEQ/COPPE/UFRJ, Rio de Janeiro, Brasil*
[b]*National Petroleum Agency – ANP, Av. Rio Branco 65, 17th floor, 20090-004, Rio de Janeiro, RJ, Brazil*

Received 17 April 2007; accepted 17 April 2007

This work aims at studying the effect of CO_2 addition in the non-oxidative conversion of methane over a Mo-containing MCM-22 zeolite. Catalyst characterization made use of X-ray fluorescence, textural analysis, X-ray diffraction and diffuse reflectance spectroscopy. Molybdenum was present as highly condensed species with octahedral coordination, such as $(Mo_7O_{24})_6$ and MoO_3 species. Catalytic tests were carried out at atmospheric pressure and 700 °C, with WHSV of $90 g_{CH4} \cdot g_{Mo}^{-1}\ h^{-1}$. Coke species were studied by thermogravimetric analysis and thermoprogrammed oxidation. Besides the carbidic carbon, two other types of coke were observed: one associated to molybdenum and the other associated to Brönsted acid sites located both on the catalyst surface and inside zeolite pores. The species associated to acid sites, known to be responsible for polyaromatics formation and catalyst deactivation, were reduced in a more significant way by the use of CO_2, increasing the catalyst stability.

KEY WORDS: methane; carbon dioxide; MCM-22; zeolite; molybdenum.

1. Introduction

Methane, the major component in natural gas is attracting a growing commercial interest, especially due to the recent natural gas discoveries which increased its production all over the world. Some methane conversion routes have been studied, aiming at obtaining high-value products, either for energy-generating purposes (such as Fischer-Tropsch diesel, dimetil ether and methanol) or as chemicals (such as formaldehyde and aromatics).

Methane catalytic conversion can be done through direct or indirect routes. The direct conversion into aromatics was first mentioned by Wang *et al.* [1], in 1993. Through this route, methane was converted into benzene and other aromatic hydrocarbons over a transition metal supported on a HZSM-5 zeolite under non-oxidative conditions [1–5]. The non-oxidative conversion produces both high purity hydrogen and liquid aromatic hydrocarbons, which makes their separation easier in an industrial process. From all aromatic hydrocarbons produced, the most attractive one is benzene.

Its worth to mention that the major difficulty observed is the rapid catalyst deactivation by coke deposition on the active sites. To minimize this effect, a great number of studies have been done with different transition metals [3,5–9] and different zeolites [9–14], searching for a selective catalyst for aromatics (especially benzene) but more stable than HZSM-5. One of the most promising zeolites seems to be HMCM-22 which showed a moderate deactivation even after 24 h TOS [10,11,15,16]. Some other studies tried to reduce the observed MoZSM-5 deactivation by the introduction of other gases along with methane, such as CO or CO_2 [5,16,17], H_2 [9,17–19], NO [20] and O_2 [20].

In this work, a Mo-impregnated HMCM-22 zeolite was used in the non-oxidative methane dehydro-aromatization. Carbon dioxide was fed together with methane in order to limit coke deposition by means of the Boudart reaction.

$$CO_2 + C \leftrightarrow 2CO \quad (1)$$

2. Experimental

2.1. Catalyst preparation

The HMCM-22 zeolite (SAR = 27) was synthesized according to [21] and will be referred to as MCM. The sample was dried and calcined at 550 °C for 10 h (1 h under N_2 and 9 h under air). The zeolite was impregnated (incipient wetness) with an aqueous solution of ammonium heptamolybdate to obtain a sample with 4% Mo (w/w). The resulting material was calcined at 500°C for 6 h.

*To whom correspondence should be addressed.
E-mail: acamacho@anp.gov.br

1011-372X/07/0900–0166/0 © 2007 Springer Science+Business Media, LLC

2.2. Catalyst characterization

The chemical composition was determined by X-ray fluorescence spectrometry in a Rigaku spectrometer. BET specific surface areas, micro- (t-plot) and mesopore (BJH) volumes were determined by N_2 adsorption at 77 K, in a Micromeritics ASAP 2000, after treating the samples at 300 °C for 18 h under vacuum. XRD data were taken in a Rigaku Dmax Ultima + diffractometer with CuKα radiation, 40 kV and 40 mA. The diffractogram was recorded from 5 ° to 40 ° with 0.05° steps (2 s).

Diffuse reflectance spectra (DRS) were taken with a Varian Cary 5 spectrometer equipped with a diffuse reflectance accessory, a pretreatment chamber and a computer interface for data acquisition. MCM-22 zeolite was used as reference for sample Mo4MCM.

The absorption edge and the condensation degree of the molybdenum species on the catalysts were calculated by the use of the methodology proposed by Weber [22], for bulk molybdenum compounds and for Mo supported catalysts.

From the diffuse reflectance spectra the energy on the absorption edge was determined from the intersection of a straight line fit to the curve$[(F(R_\infty)\cdot h\nu]^2$ versus $h\nu$, where $F(R_\infty)$ is the Kubelka-Munk function and hν is the incident photon energy.

The oxidation of the coke formed during methane dehydrogenation was studied by termogravimetric (TGA) and termodiferential analyses (DTA) under synthetic air flow and by termoprogrammed oxidation (TPO) under 5% O_2/He flow.

TG and DSC profiles were recorded in a Rigaku TAS 100. The catalyst was heated from room temperature to 750 °C at a heating rate of 10 °C min^{-1} in air (60 mL min^{-1}). From the TG profiles, the corresponding derivative thermogravimetric (DTG) profiles were derived.

TPO was performed from room temperature to 800 °C, using a heating rate of 5 °C min^{-1} and keeping at 800 °C for 0.5 h. The outflowing gases were also accompanied by on-line mass spectrometry (model PRISMA-QMS 200). The release of water (m/z = 18), oxygen (m/z = 32), carbon monoxide (m/z = 12 and 28) and carbon dioxide (m/z = 12, 28 and 44) was monitored. Quantification of the total amount of coke was done by using adequate calibration standards for CO and CO_2 after proper correction of the contribution of CO_2 to the signal at m/z = 28 by means of the fragmentation pattern of this compound.

2.3. Catalytic performance

The catalytic tests were performed in a quartz tubular fixed-bed microreactor either with pure methane at atmospheric pressure and 700 °C at a space velocity of 90 g_{CH4} g_{Mo}^{-1} h^{-1} or with the addition of a CO_2 stream at a space velocity of 10 g_{CO2} g_{Mo}^{-1} h^{-1} (CH_4/CO_2 molar ratio of 25). Before the catalytic tests, the samples were pretreated in N_2 at 500 °C for 2 h. Then, the samples were activated in a H_2/CH_4 mixture (5:1) from ambient temperature to 650 °C (2 h). The activation conditions were optimized by the use of mass spectrometry (Prisma, Balzers).

Hydrocarbons, such as methane, C_2H_4, C_2H_6, benzene, toluene, and naphthalene, were analyzed by on-line FID gas chromatography, while the hydrogen formed was analyzed by on-line TCD gas chromatography.

3. Results and discussion

3.1. Catalyst characterization

X-ray fluorescence confirmed that the MoMCM sample had a silica/alumina ratio (SAR) of 27. The specific surface area and the microporous volume agreeded with reported values.

The introduction of molybdenum species was adequate, with the obtention of a sample with 4% (w/w), as expected. No significant loss of crystalinity was observed as a result of Mo species introduction, with only a slight reduction of specific surface area and microporous volume, when compared with the zeolite before molybdenum impregnation.

The X-ray diffraction patterns showed a good dispersion of molybdenum species since no other phase (such as molybdenum oxide) besides HMCM-22 could be observed [15].

3.2. Mo condensed species

The diffuse reflectance spectrum, is shown in figure 1A. It can be observed a charge transfer band around 300 nm, a value close enough to that observed for MoO_3, indicating an increased polymerization degree, as observed for samples with higher Mo contents [22,23]. In order to corroborate Mo coordination in the analyzed sample, the previously described methodology proposed by Weber [22] was used.

The calculated value for the energy on the adsorption edge was 3.59 eV (figure 1B), confirming the presence of MoO_3 species (octahedral coordination) (energy of the edge close to 3.40 eV) [23]. The difference between the mentioned values suggests the presence of other condensed species, besides MoO_3, such as $(Mo_7O_{24})_6$ with octahedral coordination and energy on the adsorption edge of 3.70 eV.

This result is somewhat different from that observed for HZSM-5 zeolite, when MoO_3 species were present only over samples with Mo contents higher than 4% (w/w). This difference can be attributed to the presence of cavities in HMCM-22, when compared to HZSM-5 zeolite.

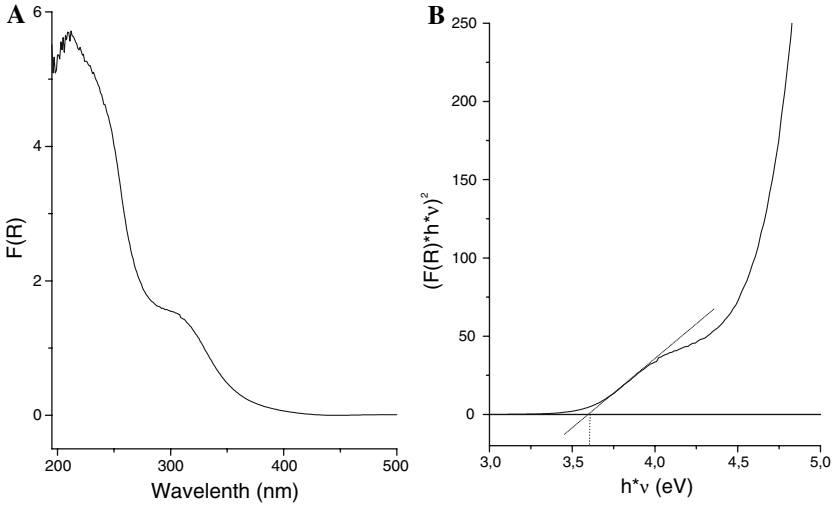

Figure 1. (A) Diffuse reflectance spectra of Mo4MCM and (B) Energy on the adsorption edge on Mo4MCM.

3.3. Non-oxidative methane dehydroaromatization

The non-oxidative methane dehydrogenation products observed were hydrogen, C2 species (ethane and ethylene), benzene, toluene, naphthalene, and polycondensed hydrocarbons.

The performance of sample Mo4MCM with and without the use of CO_2 on the feedstock is shown in figure 2A and B.

The experiment performed without the use of CO_2 showed a high initial conversion (10%), similar to that observed for HZSM-5 zeolite, which decreased along the run, reaching 5.3% after 25 h TOS. It can be observed the predominance of benzene among the products. After that initial period, both benzene and naphthalene selectivities stay almost constant. It is interesting to report that toluene and policondensed hydrocarbons selectivities were close to 3% and 4%, respectively, during the catalytic tests.

The use of CO_2 in the feedstock improved the stability of the catalyst as compared to the feed of pure methane, with the conversion varying from 6.7% to 5.7% along the run, although the initial conversion was lower. As to the selectivities, no difference in benzene selectivity was observed, although an increase in naphthalene selectivity and a decrease in toluene and polycondensed hydrocarbons selectivities to negligible values was observed.

3.4. Coke characterization

After dehydro-aromatization of methane, the coked samples were submitted to thermal treatment as previously described (TGA). The TGA profiles are shown in figure 3.

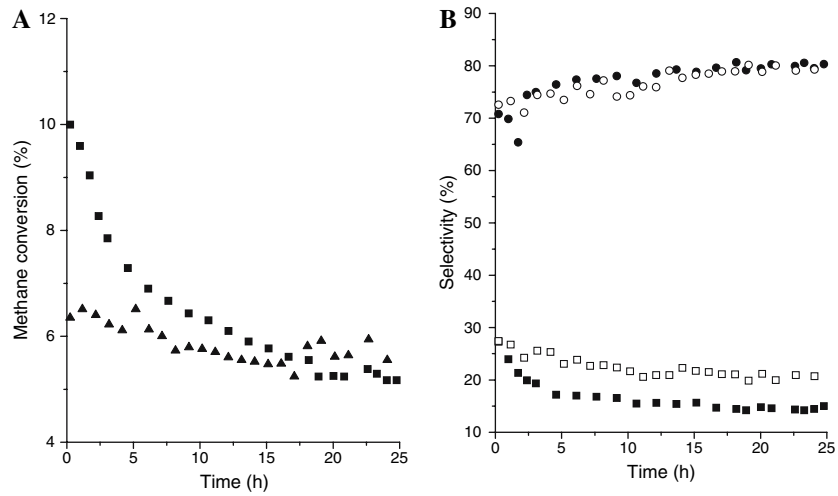

Figure 2. Catalytic performance. (A) Methane conversion (■ – without CO_2 e▲– with CO_2) and (B) Benzene and naphthalene selectivities (■ ● – without CO_2, □ ○ – with CO_2, ● ○ – benzene, ■ □ – naphthalene.

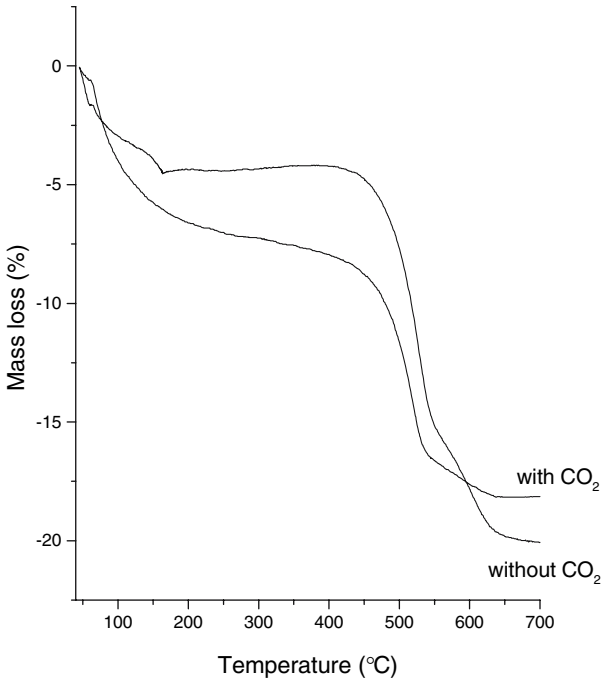

Figure 3. Termogravimetric profile of Mo4MCM after reaction, with and without CO_2.

The TGA profile of the coked sample in absence of CO_2 showed initial loss attributed to the desorption of physisorbed water from the zeolite pores. After the loss of water, an increase in mass weight can be related to the conversion of molybdenum carbide into molybdenum oxide (IV). Mass loss after carbide oxidation can be attributed to the burning of coke. So, it became evident that carbon species have two distinct natures (carbidic and non-carbidic carbon). From the weight losses, the amount of coke oxidized in each step can be calculated. When CO_2 was present in the feed stream, water desorption was slow and covered a large temperature range, overlapping the carbide oxidation step, thus preventing the calculation of the amount of carbidic carbon. The methodology used is described elsewhere [15,17].

The results can be observed in table 1. Since the amount of carbon in carbidic form is appreciably lower than that of non-carbidic coke, it can be neglected in the discussion. The values in table 1 shows a significant decrease of the deposited coke amount (34% reduction) on the catalyst when CO_2 was used in the feedstock.

The decrease of the apparent activation energy for coke burn-off when CO_2 was present in the feed (table 2) indicates that coke deposition occurred on a lesser acidic environment suggesting that the decrease of the amount of coke associated to Brönsted acid sites (Cb) was larger than that of the coke associated to molybdenum (Cm) (non-acidic sites), thus decreasing the ratio Cb/Cm.

From TPO analyses, as can be observed from the sum of CO and CO_2 profiles shown in figure 4, no evolution

Table 1
Amount of carbon deposits by TGA

	Water (%)	Carbidic coke (mg/g)	Non-carbidic coke (mg/g)	Total coke (mg/g)	Coke (%)
Without CO_2	4.5	0.6	198.7	199.3	19.9
With CO_2	8.4	–	131.2	131.2	13.1

Table 2
Apparent activation energies for coke burn-off from TGA results

	Activation energy (kJ mol^{-1})
Without CO_2	166
With CO_2	67

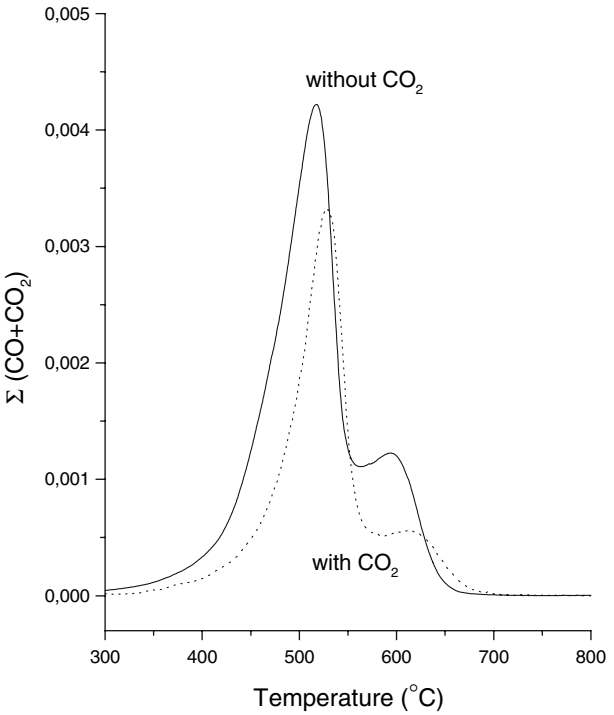

Figure 4. Termoprogrammed oxidation of Mo4MCM after reaction, with or without CO_2 in the feed (total release).

was observed until 320 °C. This indicates that no carbon burning took place below that temperature, in accordance with the TGA profiles.

The amount of coke related to each peak was determined by the combination of areas with the total amount of non-carbidic coke, as determined by TGA.

A similar study for HZSM-5 [24] also showed two peaks in the TPO profile which were ascribed to a reactive coke, probably associated to molybdenum, and to an inert or irreversible coke (claimed as responsible for deactivation and for polyaromatics formation, related to Brönsted acid sites) [25]. As already mentioned in

Table 3
Distribution of carbon deposits by TPO

	Peak 1		Peak 2	
	T (°C)	Coke (mg/g)	T (°C)	Coke (mg/g)
Without CO_2	518	156.9	590	41.8
With CO_2	528	109.8	610	21.4

Table 4
Average selectivities (25 h TOS) on the basis of methane conversion

Compound	Without CO_2	With CO_2
Benzene	74.9	75.0
Toluene	3.0	0
Naphthalene	15.8	21.6
Polycondensed	2.9	1.0
Coke	3.4	2.4

earlier studies [26], the peak with maximum between 510 °C and 530 °C can be attributed to reactive coke and the last peak, between 590 °C and 610 °C, to inert coke (table 3).

It can be observed that the decrease of the amount of deposited coke was more intense for the coke associated to the acid sites (49% reduction), decreasing from 41.8 mg/g (reaction without CO_2) to 21.4 mg/g (reaction with CO_2), which explains the higher stability and the negligible production of polycondensed hydrocarbons with the use of CO_2. These results are in agreement with the previously calculated apparent activation energies from TGA. It must be pointed that the presence of CO_2 on the feed can also inhibit the dehydrogenation of the inert coke, forming graphitic coke, responsible for catalyst death [27].

Taking methane conversion to coke into consideration, the average distribution of the products (table 4) can be evaluated. It is clear that the introduction of CO_2 in the feed reduced the amounts of toluene, polycondensed aromatics, and coke, while the amount of naphthalene increased and that of benzene was not sensitive to the different procedures used. Without the use of CO_2 in the feed, 3.4% of the converted methane was transformed into coke, while it decreased to 2.4%, when CO_2 was used in the feed.

4. Conclusions

Methane dehydro-aromatization over the bifunctional catalyst Mo-HMCM-22 with 4 wt% of molybdenum at 700 °C and atmospheric pressure showed high initial conversion (10%), comparable to that over Mo-HZSM-5. Molybdenum was present as highly condensed species. Deactivation of the catalyst was observed (especially on the first 6–7 h TOS), although in a lower extent when compared with Mo-ZSM-5. The use of CO_2 in the feedstock promoted an improvement in stability, without changing benzene selectivity. The better stability can be attributed to the reduction of coke formation, especially the inert coke, which reacted with CO_2 with CO formation. The decrease of inert coke formation also led to a lower production of polycondensed hydrocarbons.

References

[1] L. Wang, J. Huang, L. Tao, Y. Xu, M. Xie and G. Xu, Catal. Lett. 21 (1993) 35.
[2] S. Liu, L. Wang, R. Ohnishi and M. Ichikawa, J. Catal. 181 (1999) 175.
[3] B.M. Weckhuysen, D. Wang, M.P. Rosynek and J.H. Lunsford, J. Catal. 175 (1998) 338.
[4] W. Ding, G.D. Meitzner and E. Iglesia, J. Catal. 206 (2002) 14.
[5] L. Wang, R. Ohnishi and M. Ichikawa, J. Catal. 190 (2000) 276.
[6] S. Qi and B. Yang, Catal. Today 98 (2004) 639.
[7] P.L. Tan, C.T. Au and S.Y. Lai, Catal. Lett. 112 (2006) 239.
[8] X.L. Zhu, K.L. Yu, J. Li, Y.P. Zhang, Q. Xia and C.J. Liu, React. Kinet. Catal. Lett. 87 (2005) 93.
[9] R. Kojima, S. Kikuchi, H. Ma, J. Bai and M. Ichikawa, Catal. Lett. 110 (2006) 15.
[10] A.C.C. Rodrigues and J.L.F. Monteiro, Stud. Surf. Sci. Catal. 147 (2004) 709.
[11] Y. Shu, R. Ohnishi and M. Ichikawa, Catal. Lett. 81 (2002) 9.
[12] A. Martínez, E. Peris and G. Sastre, Catal. Today 107–108 (2005) 676.
[13] Y. Li, T. Wu, W. Shen, X. Bao and Y. Xu, Catal. Lett. 105 (2005) 77.
[14] L. Liu, D. Ma, H.Y. Chen, H. Zheng, M.J. Cheng, Y.D. Xu and X.H. Bao, Catal. Lett. 108 (2006) 25.
[15] A.C.C. Rodrigues and J.L.F. Monteiro, Stud. Surf. Sci. Catal. 158 (2005) 1295.
[16] J. Bai, S. Liu, S. Xie, L. Xu and L. Liu, Catal. Lett. 90 (2003) 123.
[17] Z. Liu, M.A. Nutt and E. Iglesia, Catal. Lett. 81 (2002) 271.
[18] H. Ma, R. Ohnishi and M. Ichikawa, Catal. Lett. 89 (2003) 143.
[19] H. Ma, R. Kojima, S. Kikuchi and M. Ichikawa, Catal. Lett. 104 (2005) 63.
[20] P.L. Tan, Y.L. Leung, S.Y. Lai and C.T. Au, Catal. Lett. 78 (2002) 251.
[21] A. Corma, C. Corell and J. Pérez-Pariente, Zeolites 2 (1995) 15.
[22] R.S. Weber, J. Catal. 151 (1995) 470.
[23] R.L. Martins, L.E.P. Borges and F.B. Noronha, Proc. 13th Congresso Brasileiro de Catálise, Foz de Iguaçu. (2005) Vol. 1, p. 130.
[24] H. Liu, T. Li, B. Tian and Y. Xu, Appl. Catal. A 213 (2001) 103.
[25] R. Ohnishi, S. Liu, Q. Dong, L. Wang and M. Ichikawa, J. Catal. 182 (1999) 92.
[26] A.C.C. Rodrigues and J.L.F. Monteiro, Proc. 13th Congresso Brasileiro de Catálise, Foz de Iguaçu. (2005) Vol. 1, p. 439.
[27] H. Zheng, D. Ma, X. Liu, W. Zhang, X. Han, Y. Xu and X. Bao, Catal. Lett. 111 (2006) 111.